# Supporting Information

# Homoleptic Ni(II) Dithiocarbamate Complexes as Pre-catalysts for Electrocatalytic Oxygen Evolution Reaction

Sarvesh Kumar Pal,[a] Baghendra Singh,[b] Jitendra Kumar Yadav,[a] Chote Lal Yadav,[a] Michael G. B. Drew,[c] Nanhai Singh*,[a] Arindam Indra*[b] and Kamlesh Kumar*[a]

[a] *Department of Chemistry, Institute of Science, Banaras Hindu University, Varanasi-221005, India*

[b] *Department of Chemistry, Indian Institute of Technology, Banaras Hindu University, Varanasi-221005, India*

[c] *Department of Chemistry, University of Reading, Whiteknights, Reading RG6,6AD, UK.*

*Email Address of Corresponding Authors: kamlesh.kumar@bhu.ac.in (Kamlesh Kumar)*

*arindam.chy@iitbhu.ac.in (Arindam Indra), nsingh@bhu.ac.in (N. Singh)*

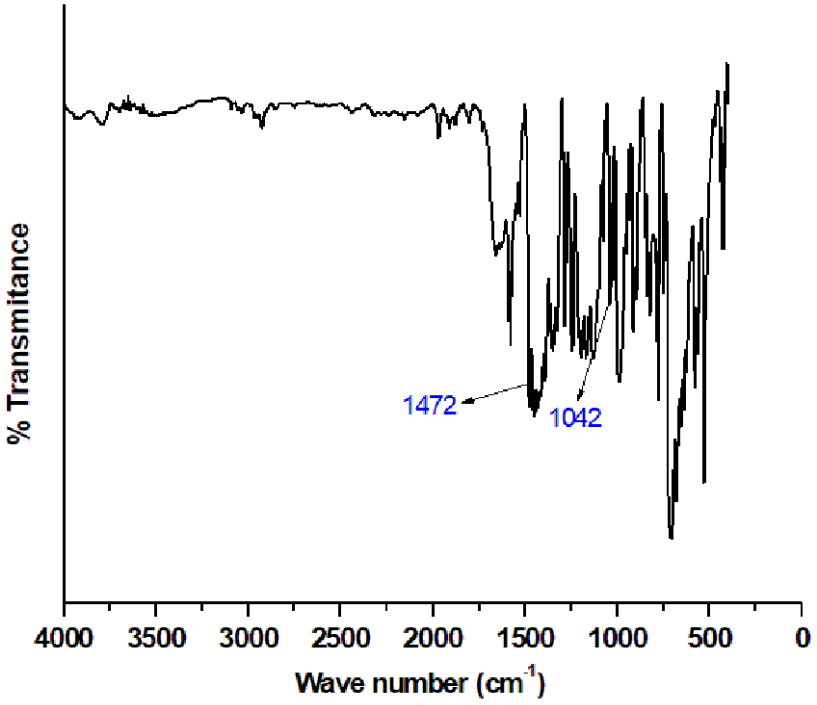


**Fig. S1a:** IR Spectrum of Ligand **KL-1.**

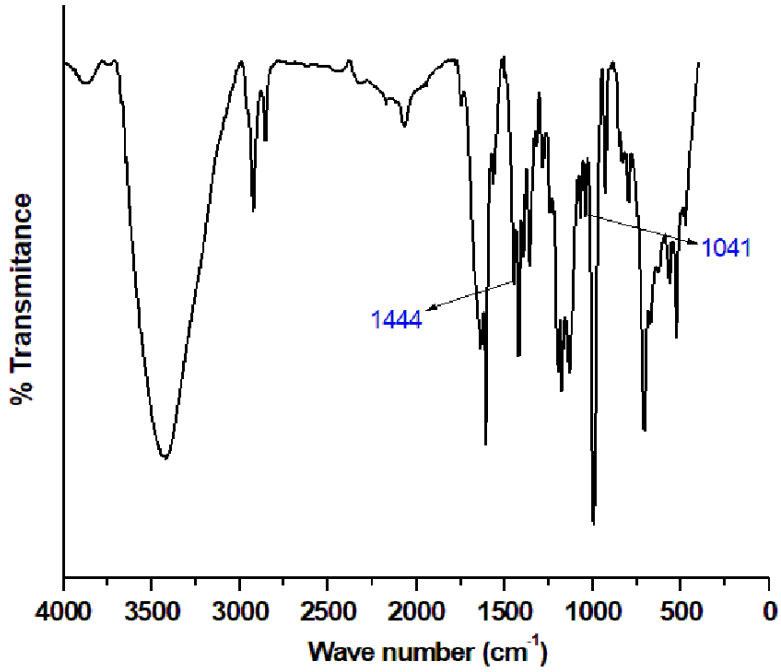


**Fig. S1b:**IR Spectrum of Ligand **KL-2**

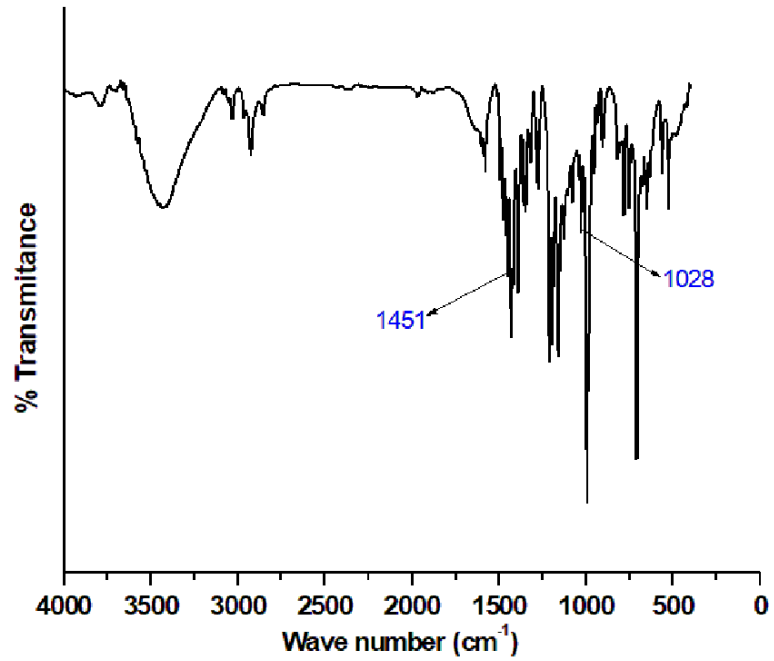


**Fig. S1c:** IR Spectrum of Ligand **KL-3**

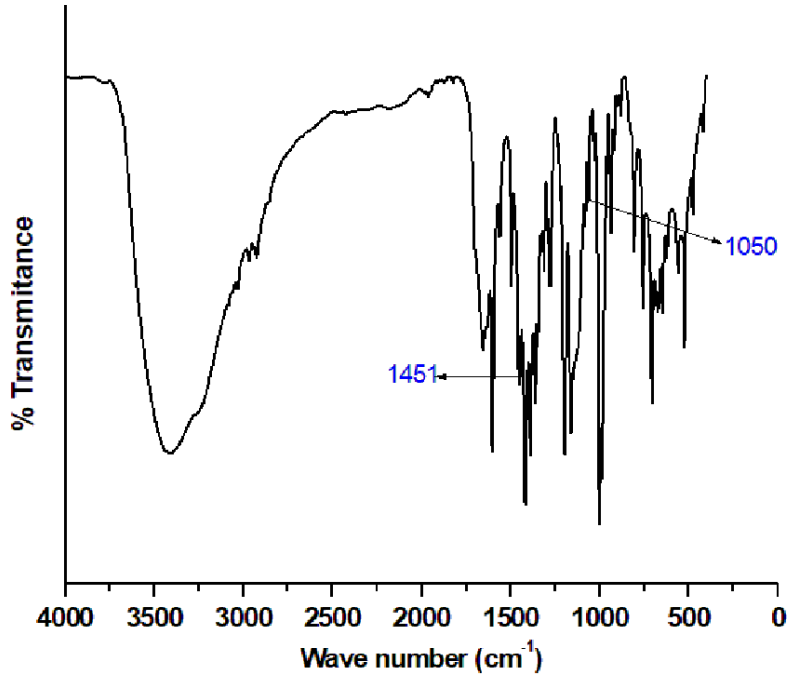


**Fig. S1d:** IR Spectrum of Ligand **KL-4**

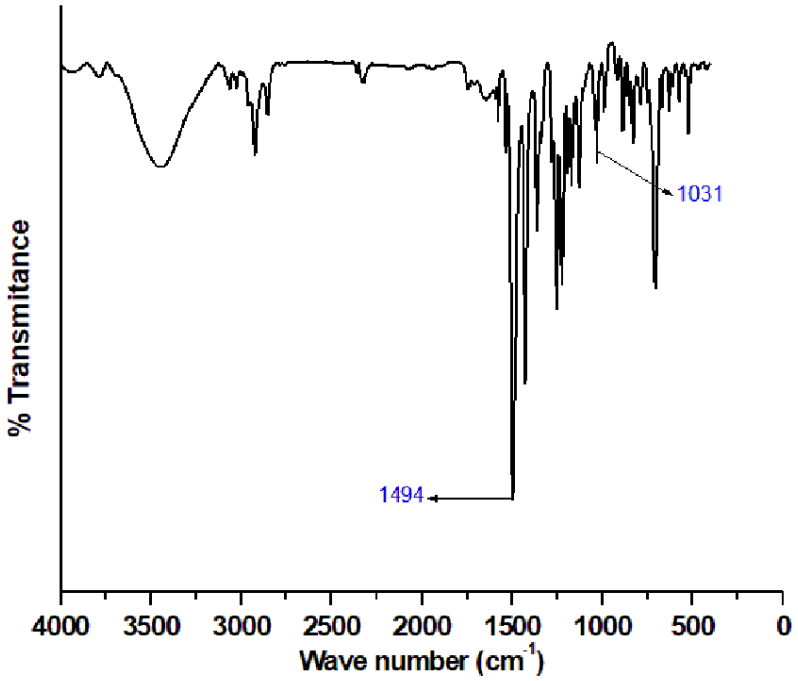


**Fig. S2a:** IR Spectrum of Complex **1**

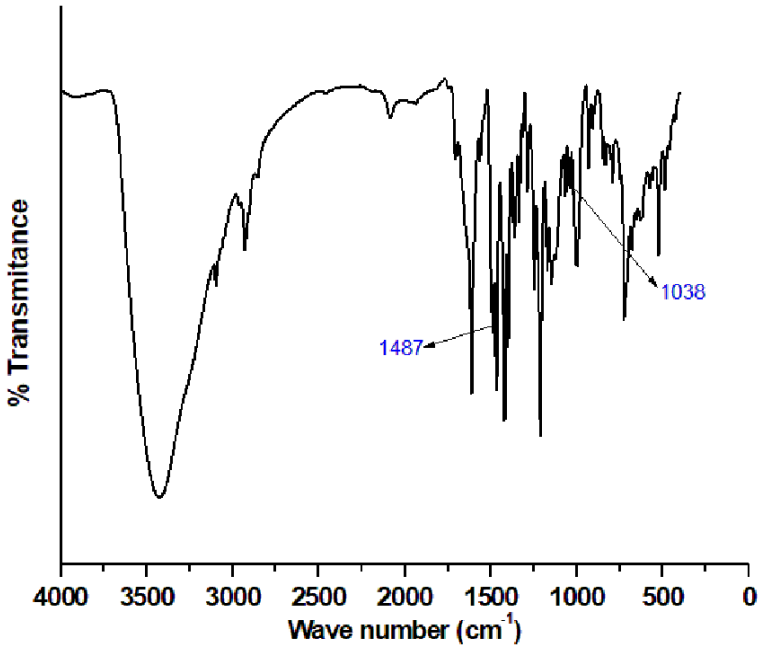


**Fig. S2b:** IR Spectrum of Complex **2**

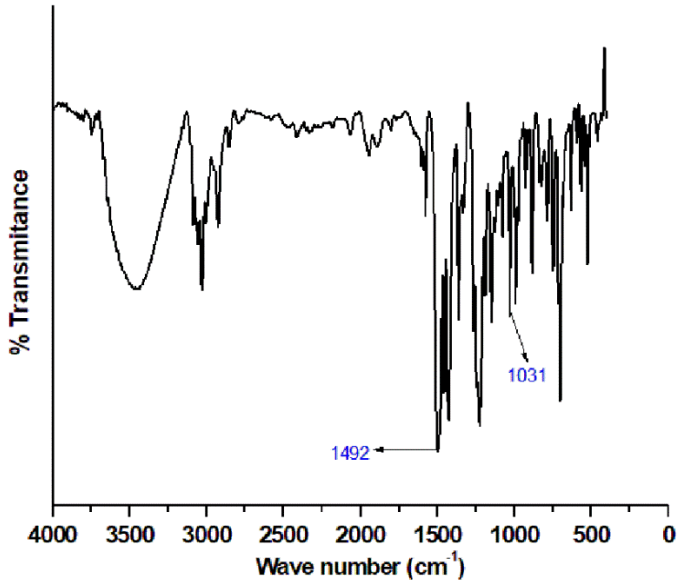


**Fig. S2c:** IR Spectrum of Complex **3**

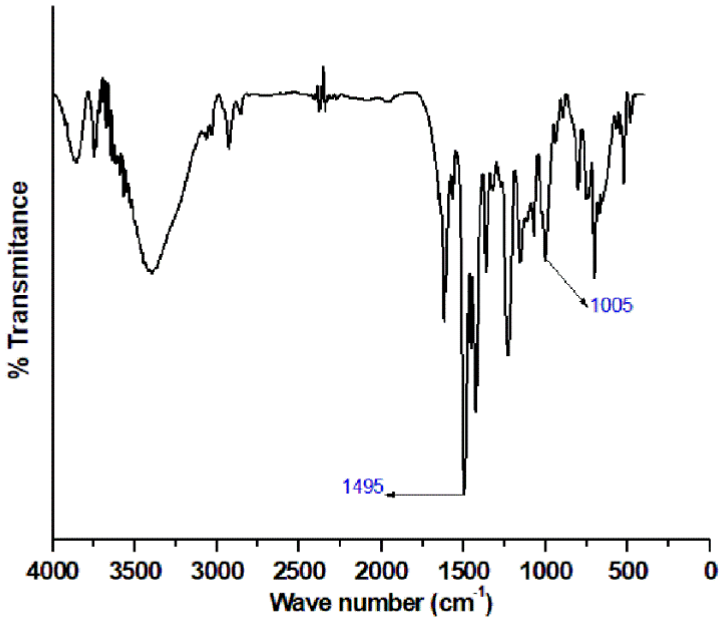


**Fig. S2d:** IR Spectrum of Complex **4**

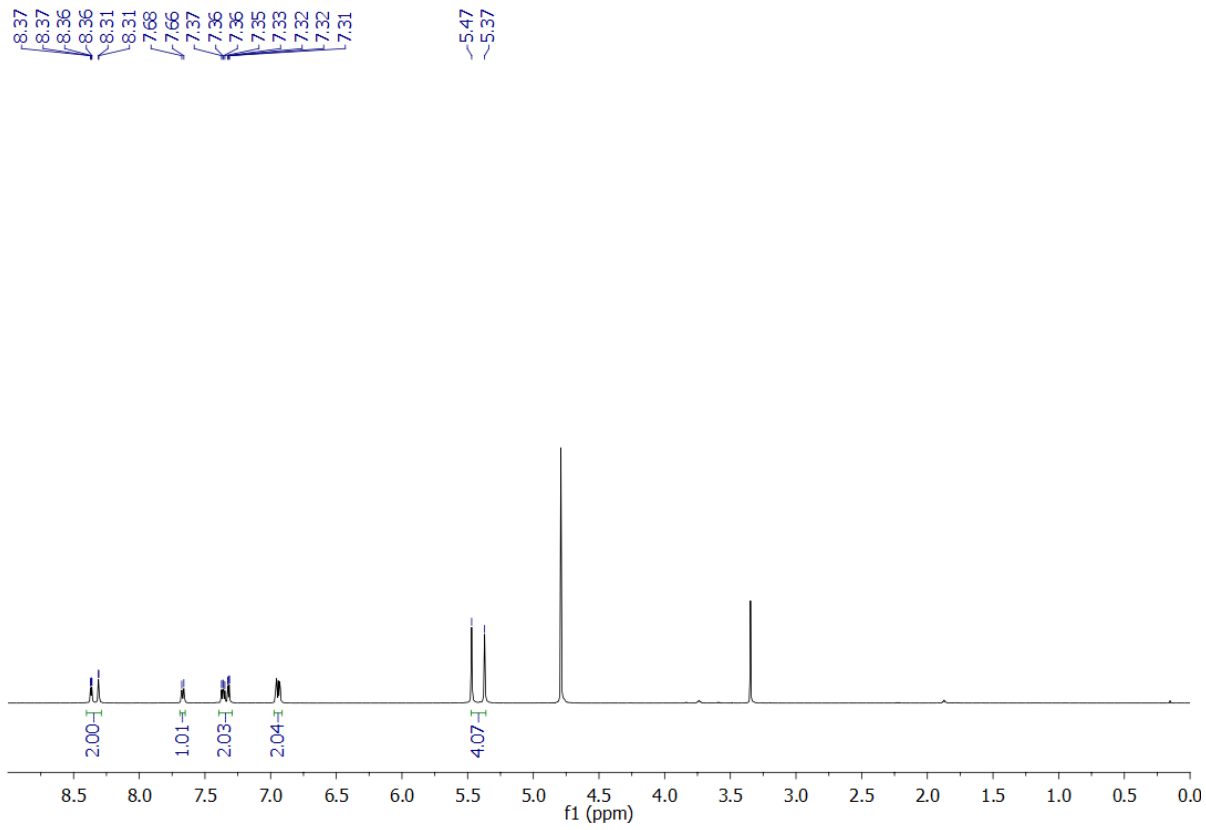


**Fig. S3a**: $^{1}H$ NMR spectrum (500 MHz, $D_2O$) of Ligand **KL-1**

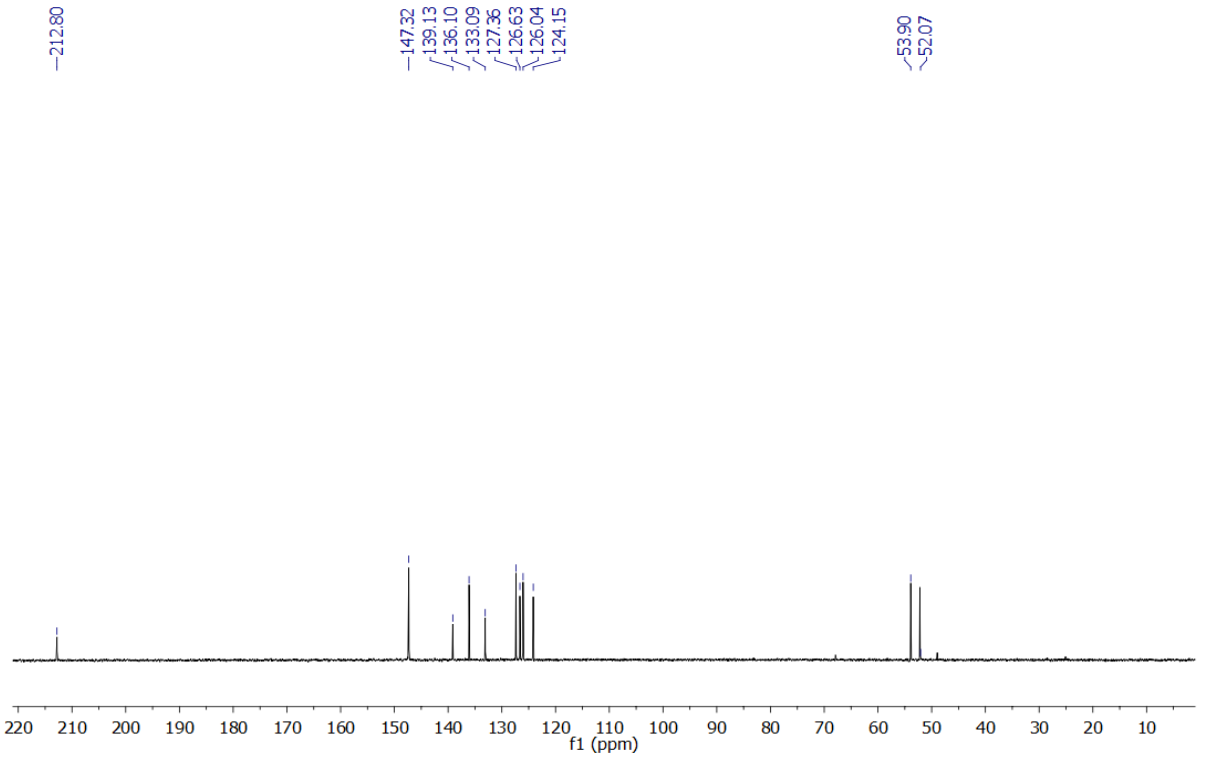


**Fig. S3b**: $^{13}C\{^{1}H\}$ NMR spectrum (125 MHz, $D_2O$) of Ligand **KL-1**

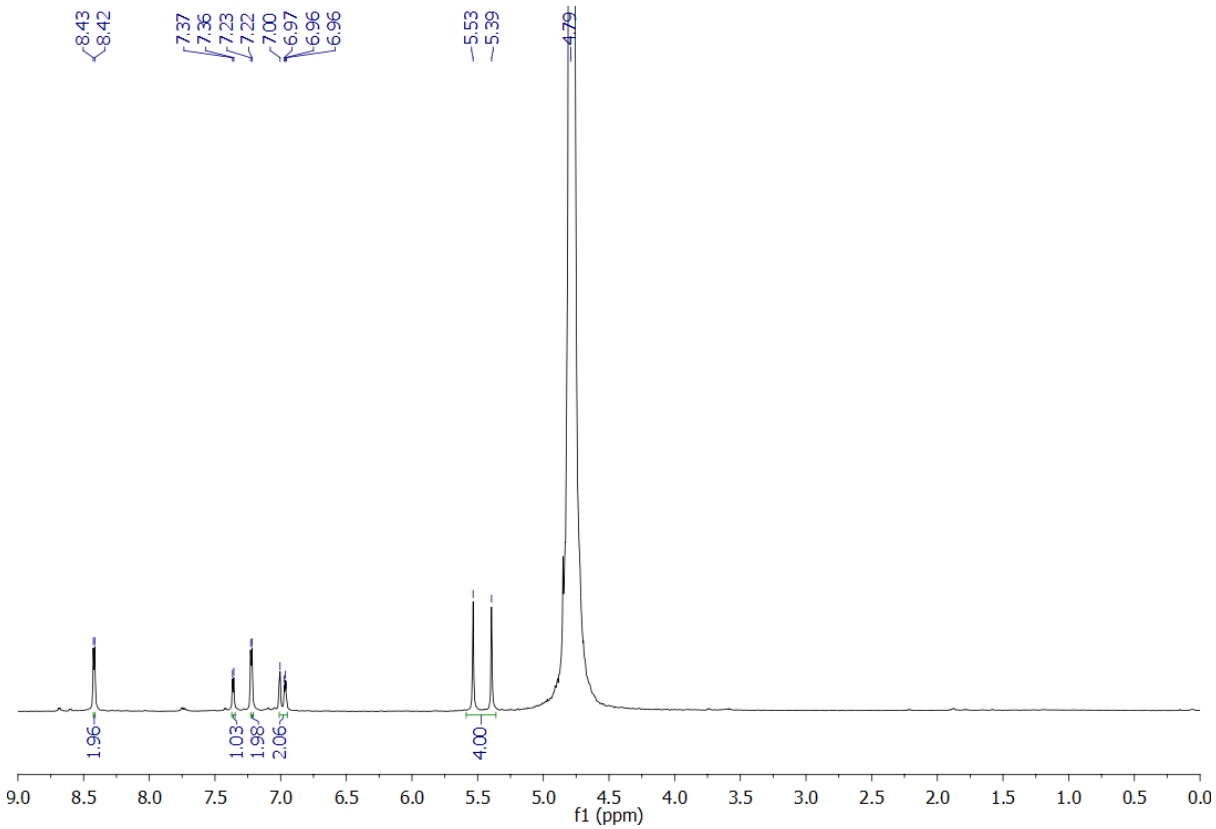


**Fig. S3c**: $^{1}$H NMR spectrum (500 MHz, $D_2O$) of Ligand **KL-2**

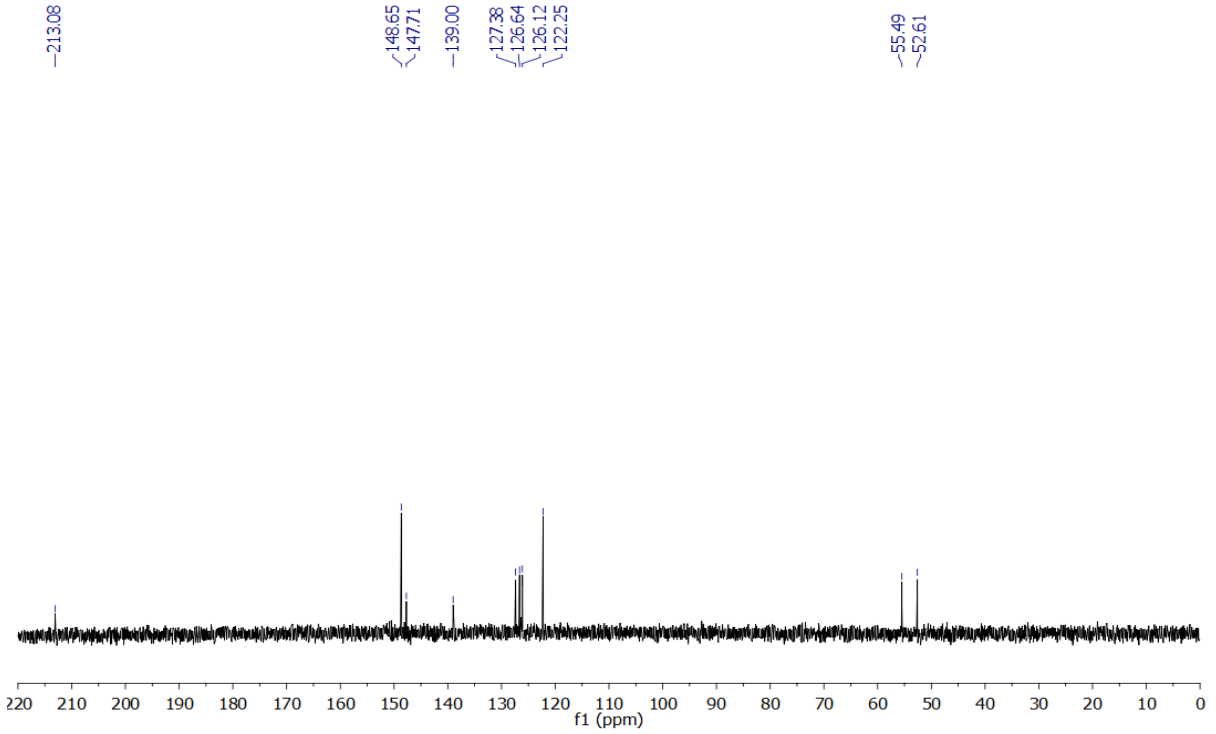


**Fig. S3d**: $^{13}C\{^{1}H\}$ NMR spectrum (125 MHz, $D_2O$) of Ligand **KL-2**

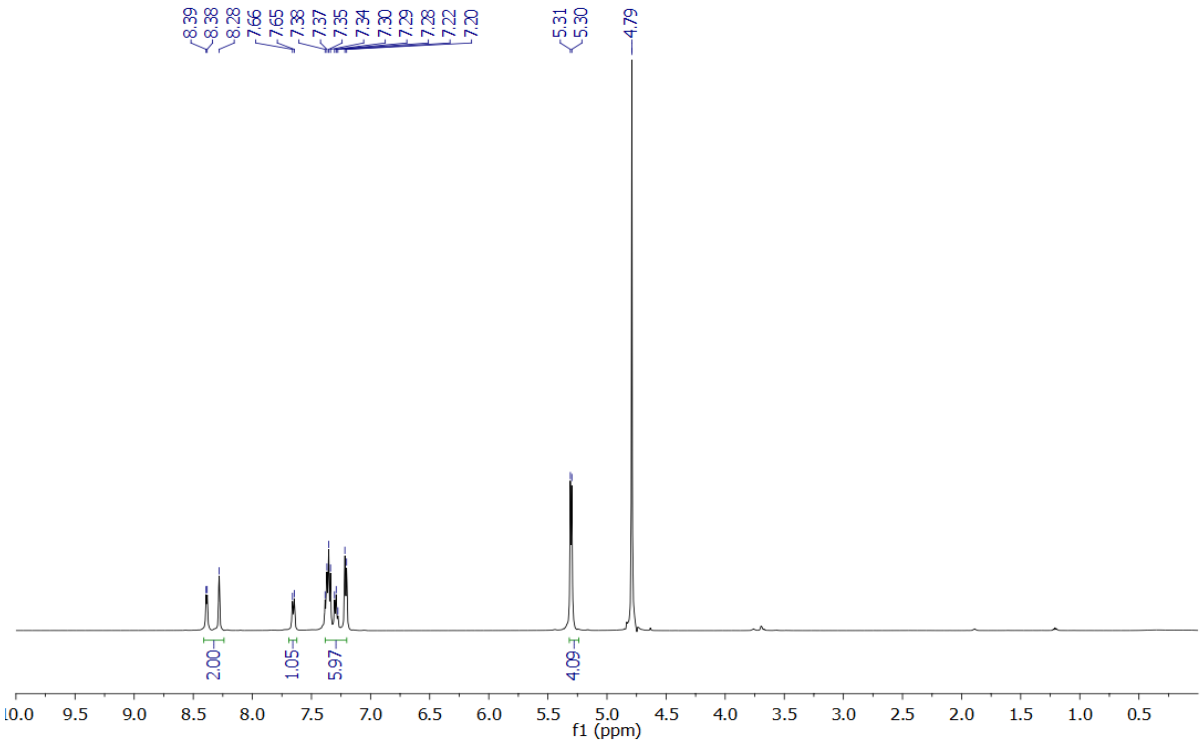


**Fig. S3e**: $^{1}$H NMR spectrum (500 MHz, $D_2O$) of Ligand **KL-3**

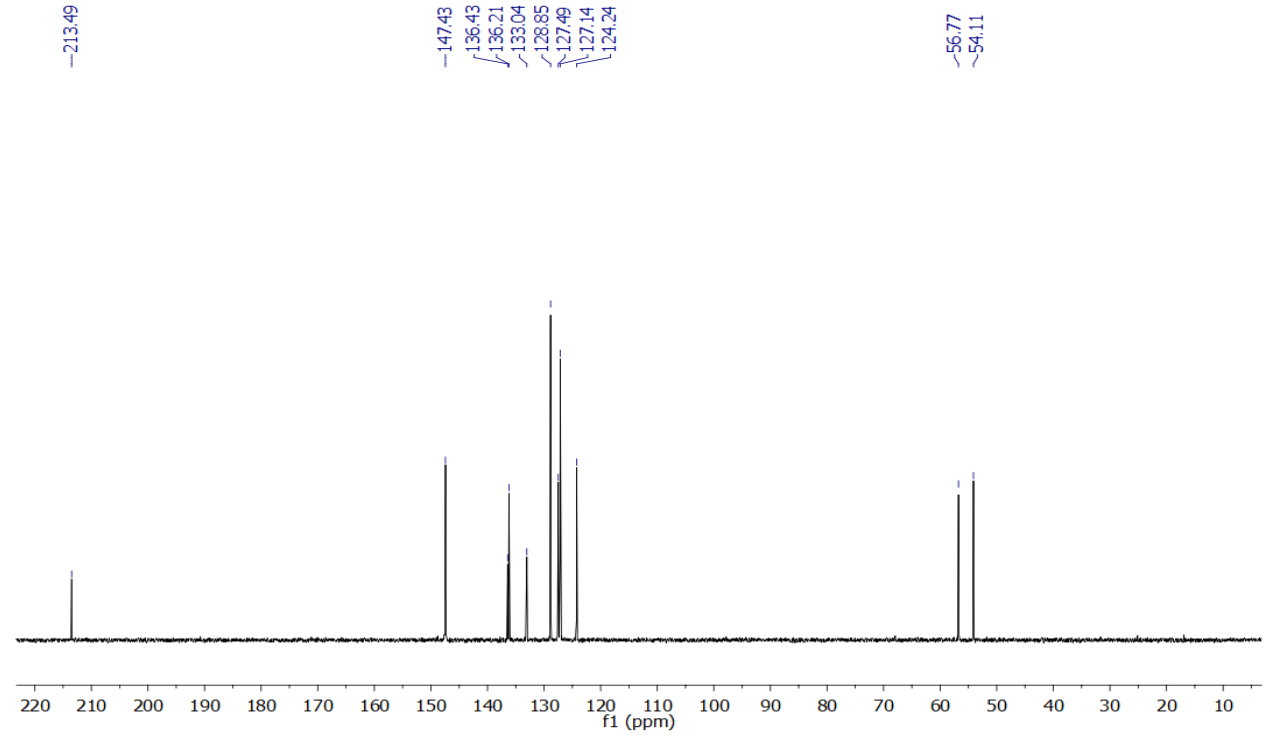


**Fig. S3f**: $^{13}C\{^{1}H\}$ NMR spectrum (125 MHz, $D_2O$) of Ligand **KL-3**

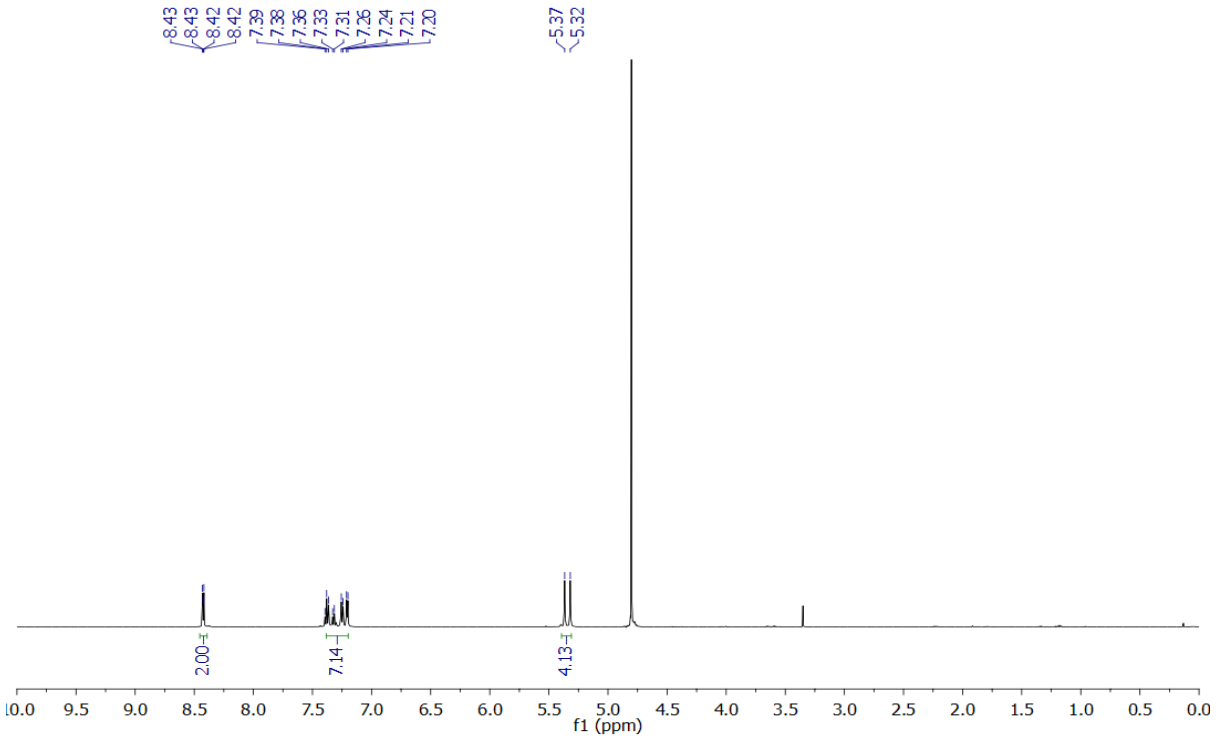


**Fig. S3g**: $^{1}H$ NMR spectrum (500 MHz, $D_2O$) of Ligand **KL-4**

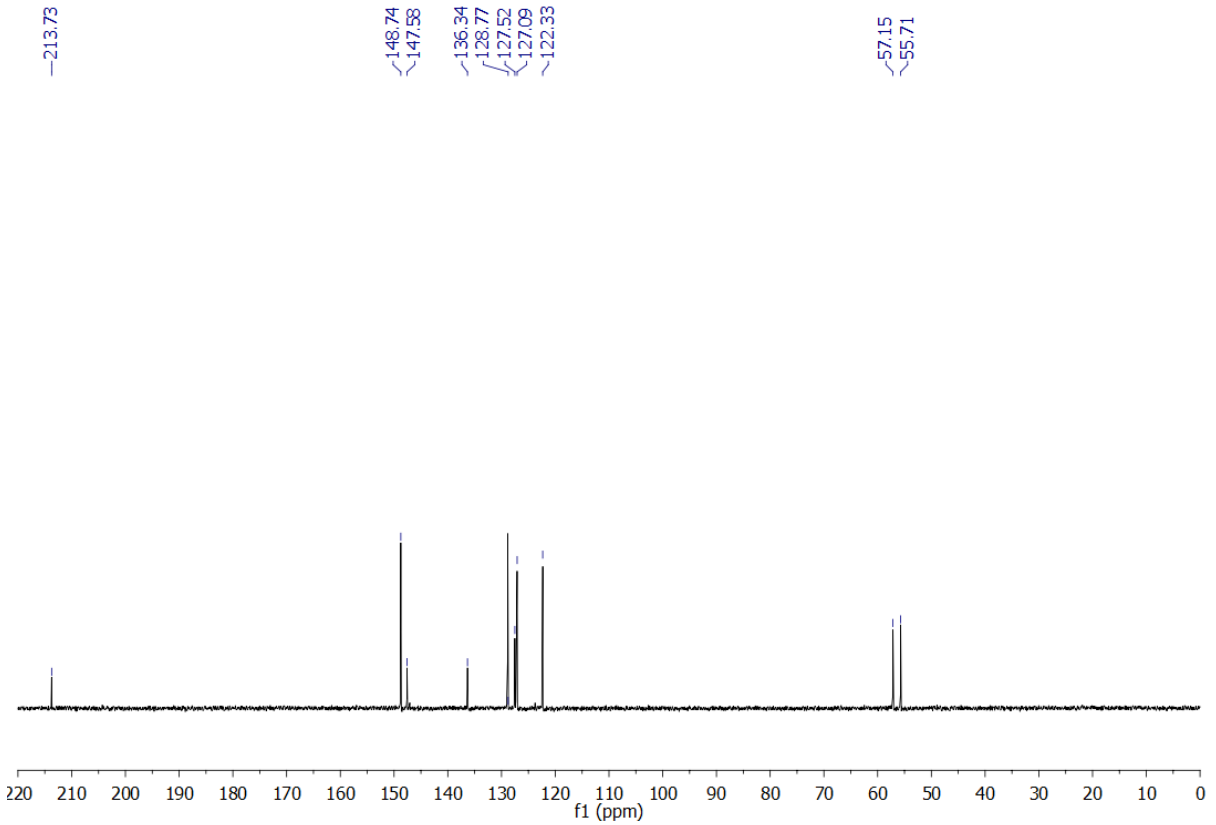


**Fig. S3h**: $^{13}C\{^{1}H\}$ NMR spectrum (125 MHz, $D_2O$) of Ligand **KL-4**

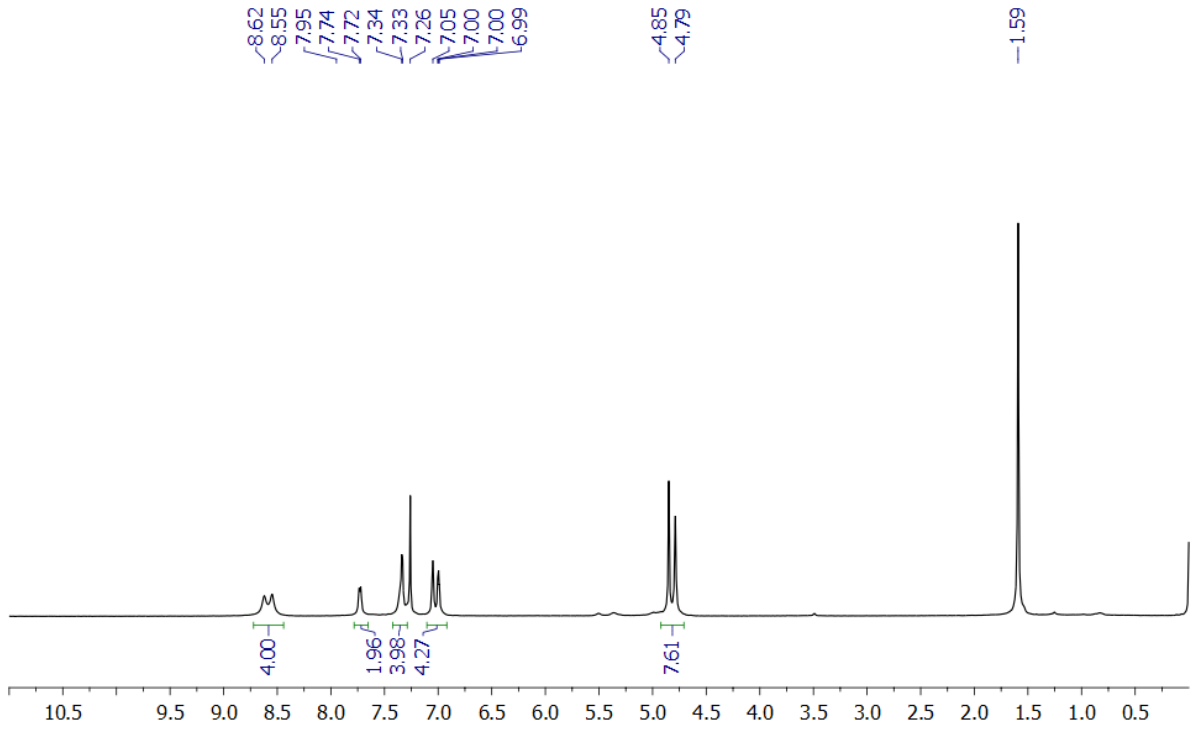


**Fig. S4a**: $^{1}H$ NMR spectrum (500 MHz, $CDCl_3$) of complex **1**

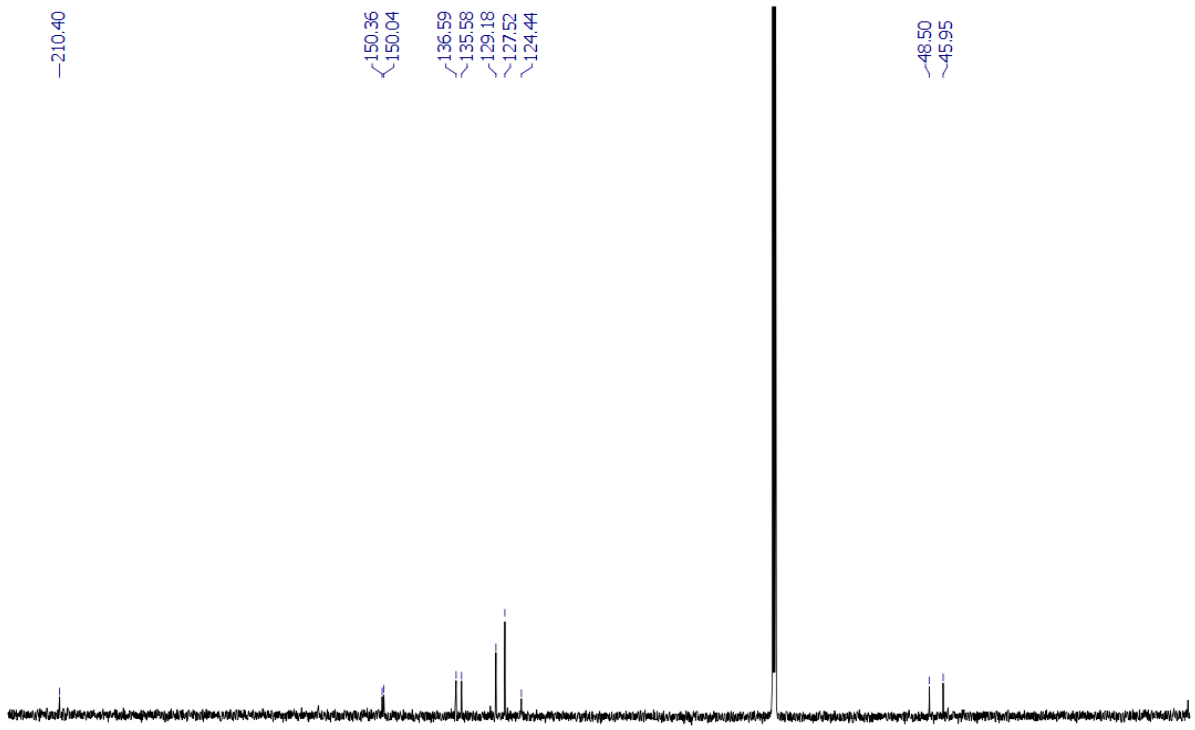


**Fig. S4b**: $^{13}C\{^{1}H\}$ NMR spectrum (125 MHz, $CDCl_3$) of complex **1**

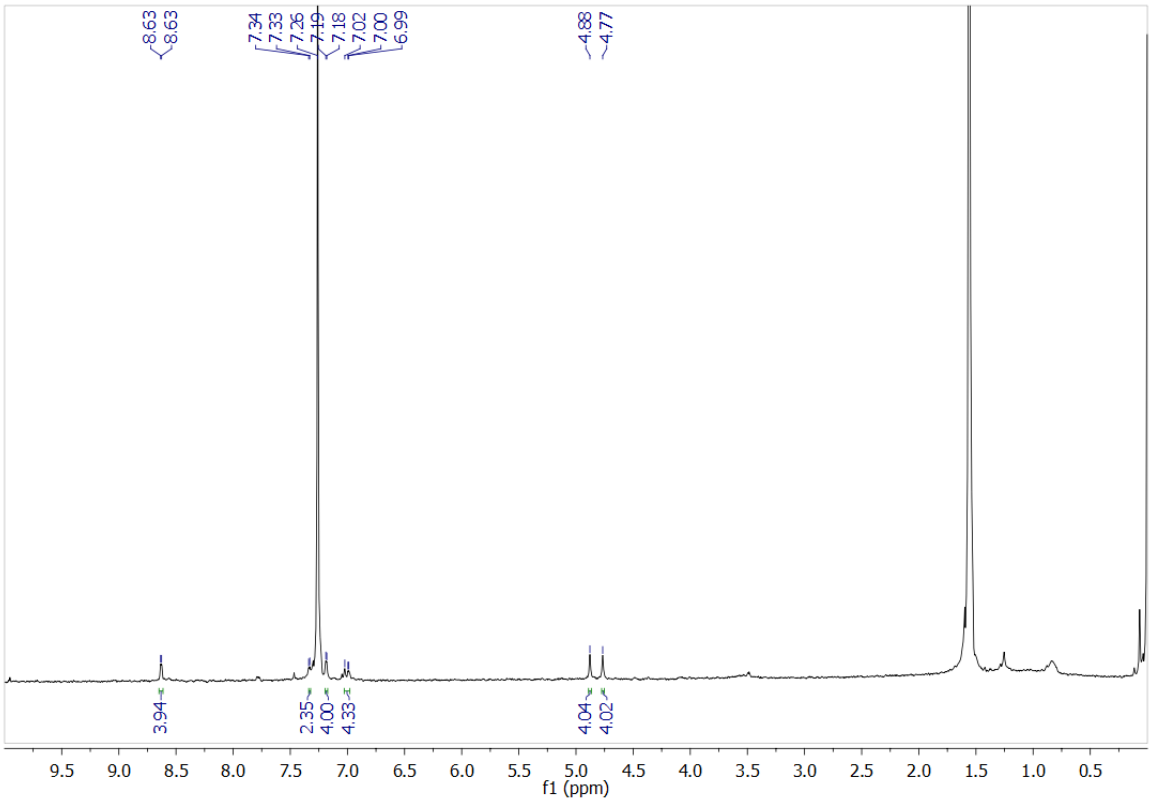


**Fig. S4c**: $^{1}$H NMR spectrum (500 MHz, $CDCl_3$) of complex **2**

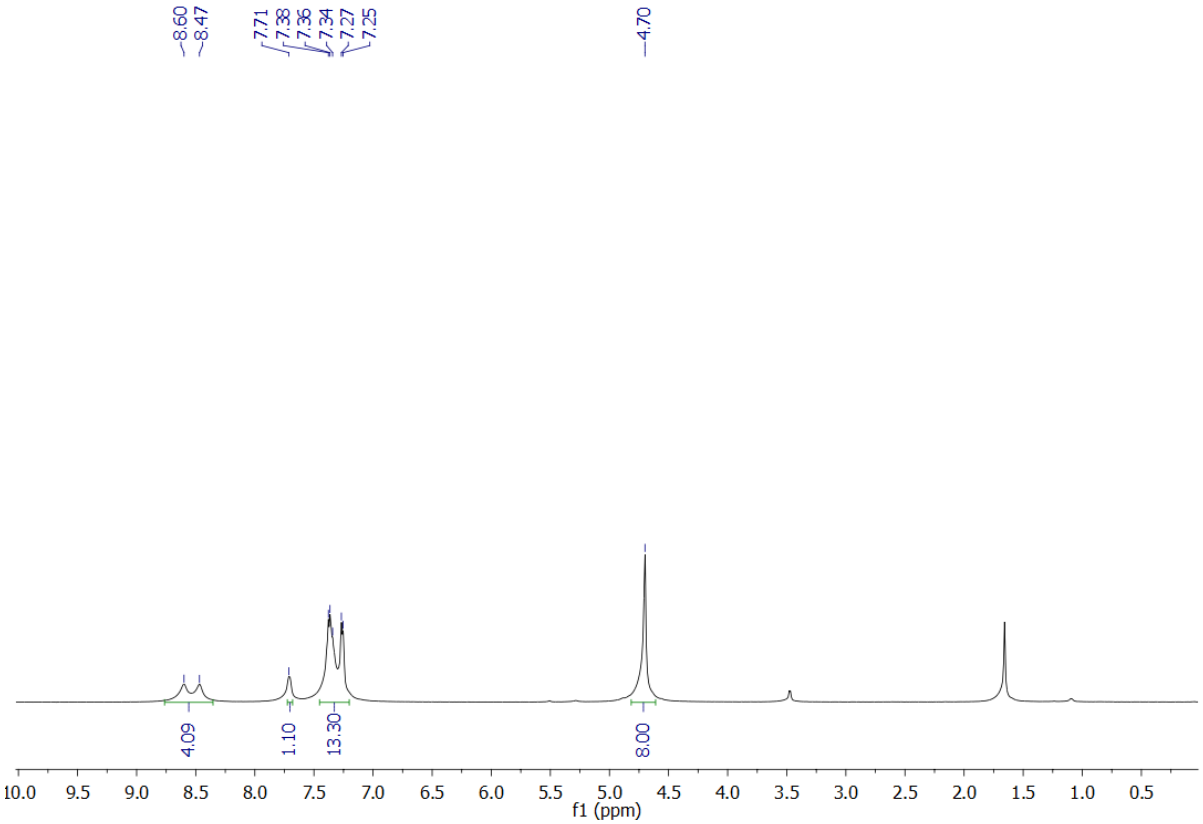


**Fig. S4d**: $^{1}$H NMR spectrum (500 MHz, $CDCl_3$) of complex **3**

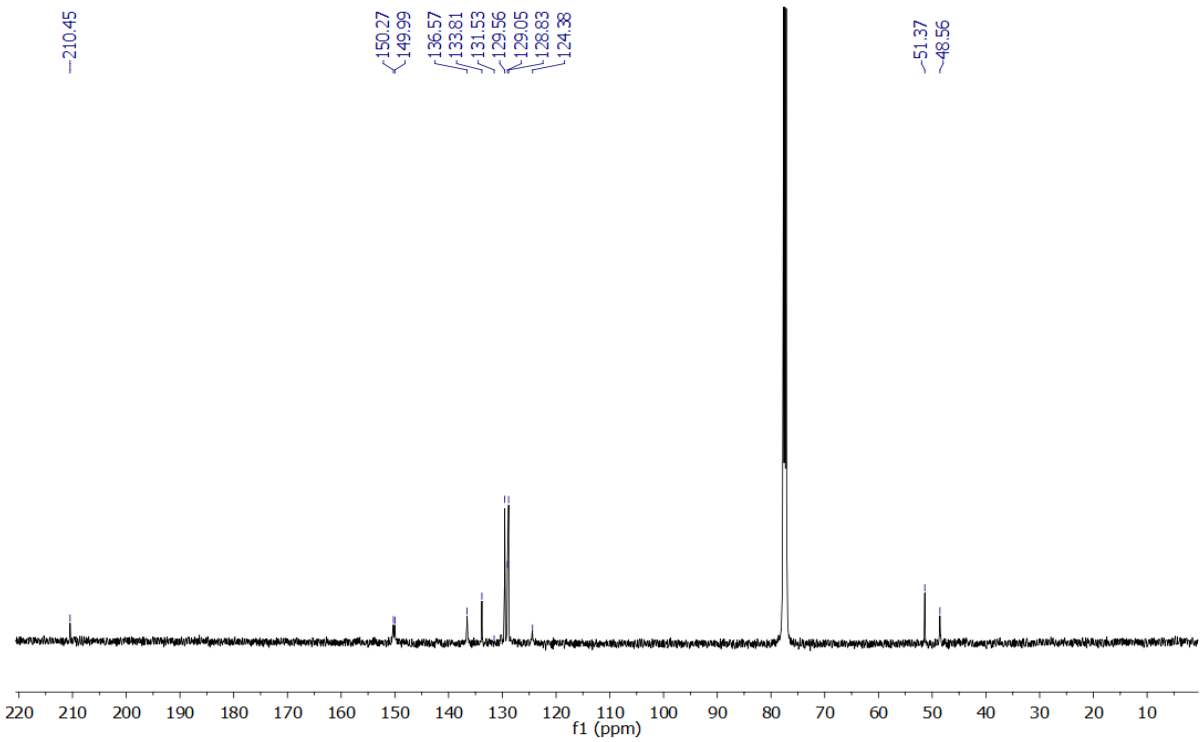


**Fig. S4e**: $^{13}C\{^{1}H\}$ NMR spectrum (125 MHz, $CDCl_3$) of complex **3**

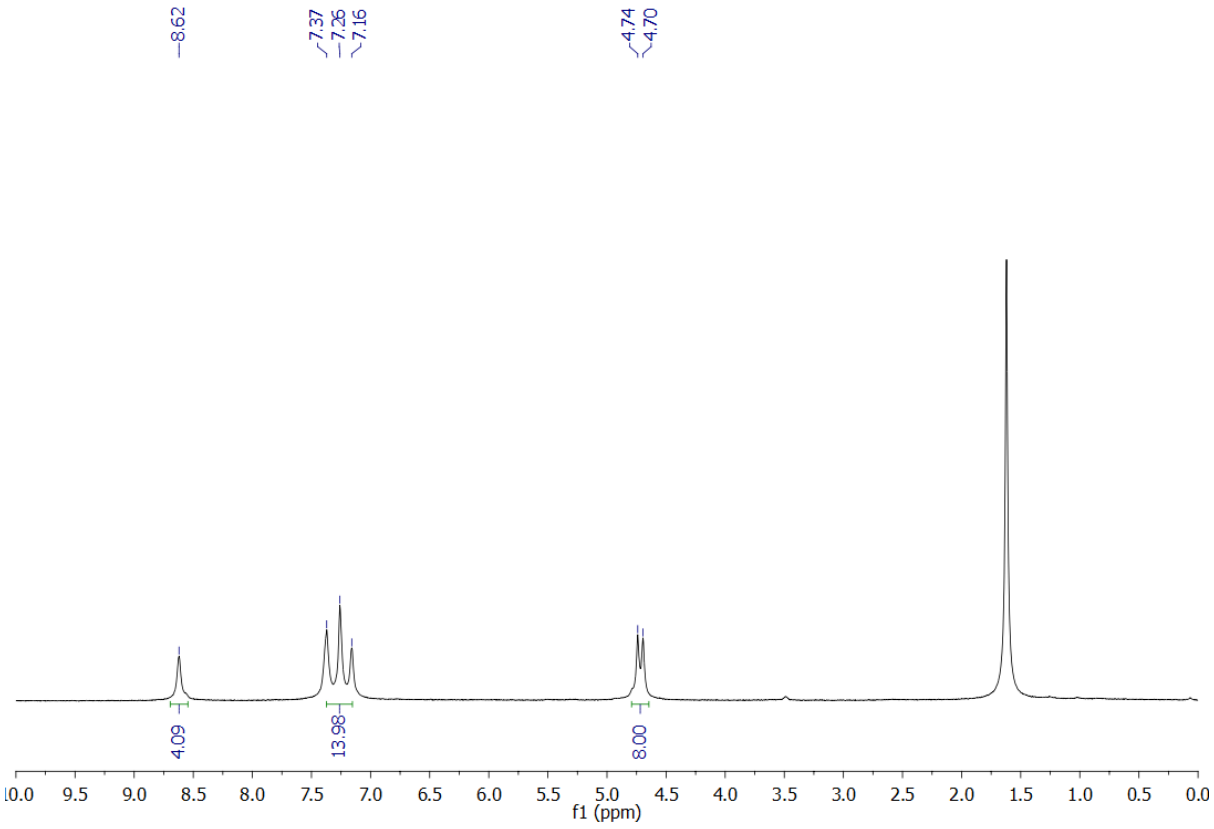


**Fig. S4f**: $^{1}H$ NMR spectrum (500 MHz, $CDCl_3$) of complex **4**

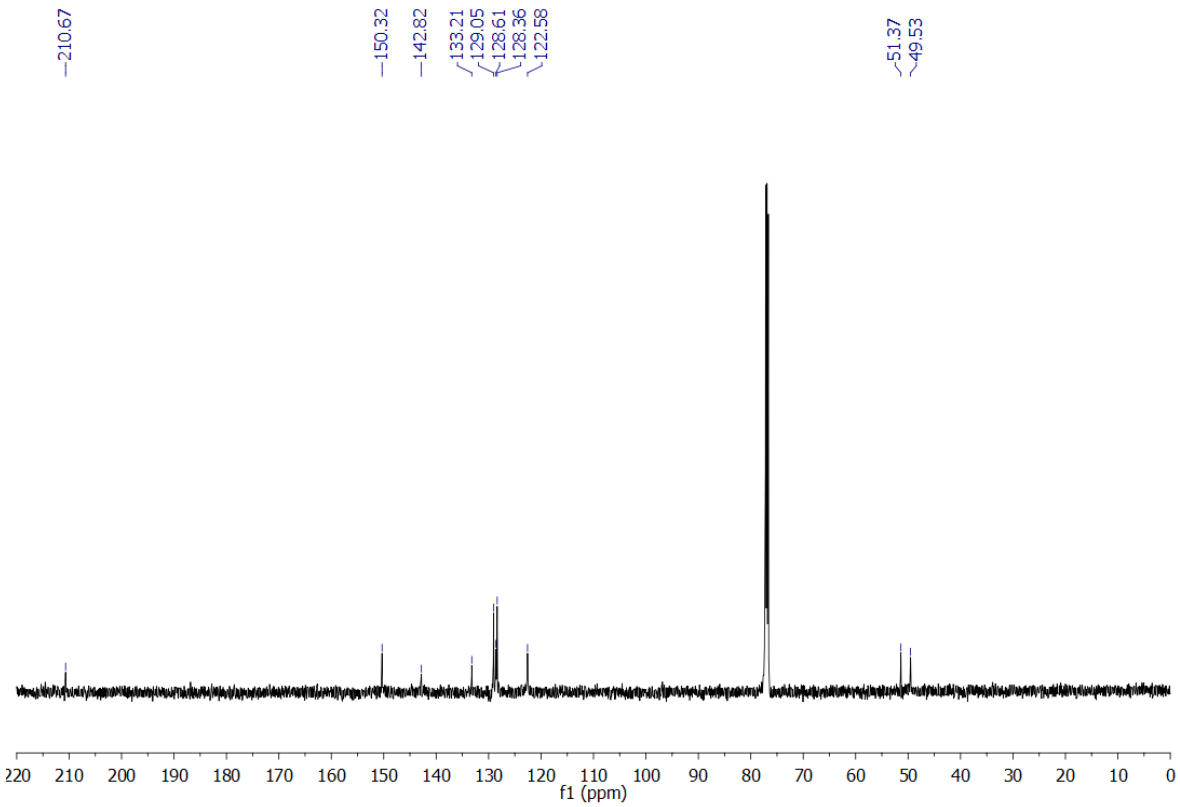


**Fig. S4g**: $^{13}C\{^{1}H\}$ NMR spectrum (125 MHz, $CDCl_3$) of complex **4.**

**Table S1.** Comparison of the OER activity of complex **2** with recently reported complexes**.**

| Catalyst[a] | Electrolyte | Overpotential (mV) | Reference |
|---|---|---|---|
| $Ni[(TMC)(CH_3CN)](NO_3)_2$ | Phosphate buffer | 590 (0.5 mA $cm^{-2}$) | Chem. Commun., 2019, 55, 6122–6125. |
| $[NiL](PF_6)_2$ | Phosphate buffer | 270 (0.65 mA $cm^{-2}$) | Catal. Sci. Technol., 2019, 9, 5651–5659. |
| Ni–Hmfchce | 0.1 KOH | 490 (10 mA $cm^{-2}$) | Polyhedron, 2019, 174, 114160 |
| Ni(II) 1,1-dithiolate-phosphine | 1 M KOH | 350 (10 mA $cm^{-2}$) | Dalton Trans., 2020, 49, 3592 |
| Cobalt Salen Complex-4 | 0.1 M potassium borate | 350 (0.1 mA $cm^{-2}$) | J. Phys. Chem. C, 2015, 119(17), 8998–9004 |
| O=PN3–Co | 0.1 M tetrabutyl ammonium perchlorate | 340 (0.5 mA $cm^{-2}$) | Inorg. Chem., 2021, 60, 614–622. |

[a] $[Ni(TMC)(CH_3CN)](NO_3)_2$: where TMC = 1,4,8,11-tetramethyl-1,4,8,11 tetraazacyclotetradecane, $([NiL](PF_6)_2$: where L = bis(2-pyridylmethylimidazolylidene) methane, Ni–Hmfchce: Nickel complex of N′-(2-methylfuran-3-carbonyl)hydrazine carbodithioic acid ethyl ester, Ni(II) 1,1-dithiolate-phosphine: Nickel complex of 2-(methylene-1,1′-dithiolato)-5,5′-dimethylcyclohexane-1,3-dione, Cobalt Salen Complex-4: Cobalt complex of 6,6′-((1E,1′E)-(ethane-1,2-diylbis(azanylylidene))bis(methanylylidene))bis-(2,4-ditert-butylphenol), O=PN3–Co: Cobalt complex of N-(di-tert-butylphosphino)[2,2′-bipyridine]-6-amine, $Co(dmgBF2)_2(OH2)_2$:BF2-annulated cobaloxime, $Co(dmgBF_2)_2(OH2)_2$ (Co-DMB, $dmgBF_2$ = difluoroboryldimethylglyoxime).

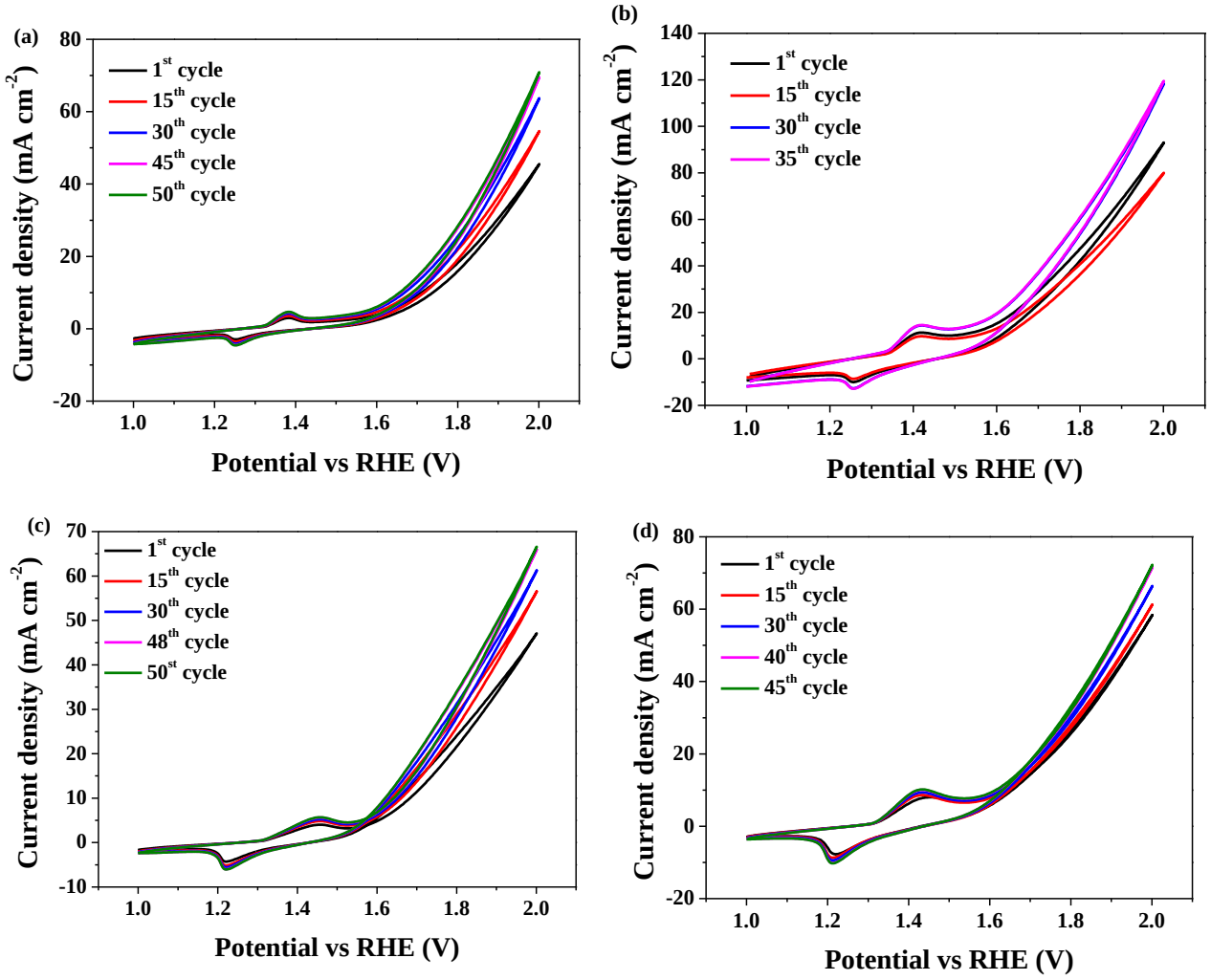


**Fig. S5**: CV profiles for the electrochemical activation of (a) complex **1**; (b) complex **2**; (c) complex **3**; and (d) complex **4** (scan rate 20 mV $s^{-1}$, without iR correction).

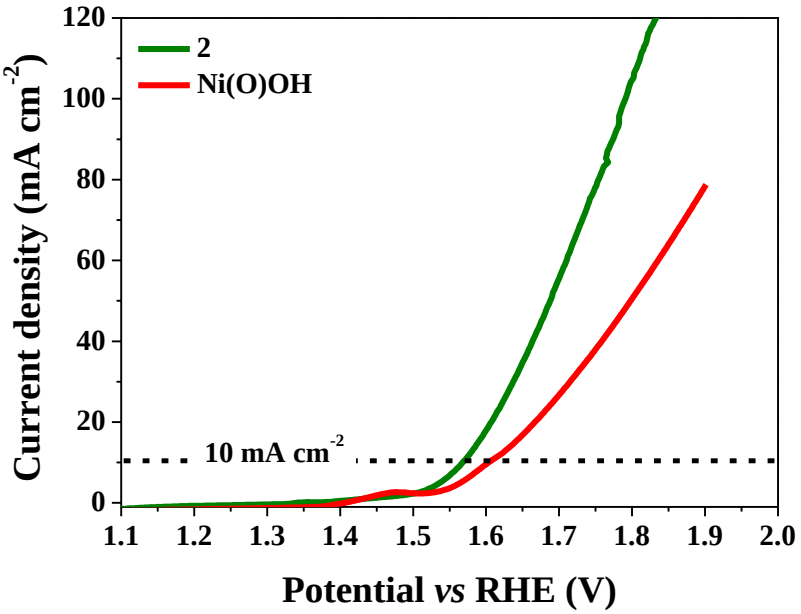


**Fig. S6**: LSV profile for the oxygen evolution reaction of complex **2**@CC compared with Ni(II) salt derived Ni(O)OH@CC in 1.0 M aqueous KOH solution. The complex **2** showed excellent OER activity compared to the Ni(O)OH (scan rate 2 mV $s^{-1}$).

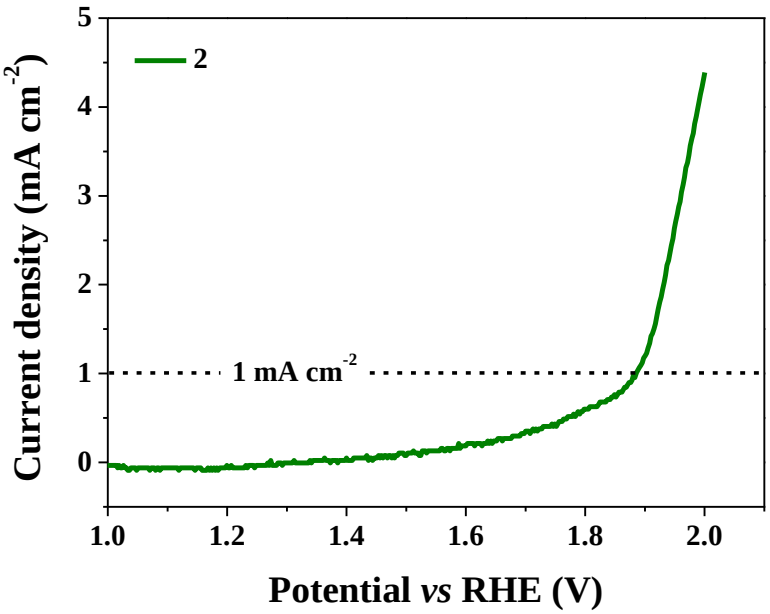


**Fig. S7**: LSV profile for the oxygen evolution reaction of complex **2** in phosphate buffer (pH = 7, scan rate = 2 mV $s^{-1}$).

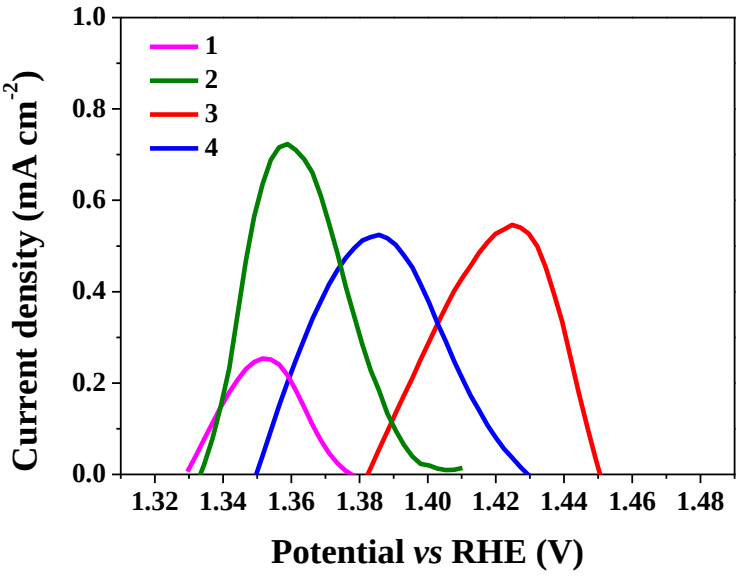


**Fig. S8:** Redox peak integration for the determination of number of active sites for the complexes **1-4**.

**Equation S1. Determination of Number of Active Sites**

The number of active sites in the complexes was calculated by the redox peak integration method.

**For complex 1**

Calculated area associated with the oxidation peak = $0.00711 \times 10^{-3}$ V A

Hence the associated charge was = $0.00711 \times 10^{-3}$ V A / 0.005 V $s^{-1}$

$= 1.42 \times 10^{-3}$ As

$= 1.42 \times 10^{-3}$ C

Now, the number of electron transferred was = $1.42 \times 10^{-3}$ C / $1.602 \times 10^{-19}$ C

$= 0.88 \times 10^{16}$

The number of electron calculated above was same as the number of surface active site due to single electron transfer involving $Ni^{2+}$/ $Ni^{3+}$ oxidation process.

Hence,

**The surface-active site of 1 that participated in OER = $0.88 \times 10^{16}$**

**For complex 2**

Calculated area associated with the oxidation peak = $0.02376 \times 10^{-3}$ V A

Hence the associated charge was = $0.02376 \times 10^{-3}$ V A / 0.005 V $s^{-1}$

$= 4.75 \times 10^{-3}$ As

$= 4.75 \times 10^{-3}$ C

Now, the number of electron transferred was = $4.75\times 10^{-3}$ C / $1.602 \times 10^{-19}$ C

$= 2.96 \times 10^{16}$

The number of electron calculated above was same as the number of surface active site due to single electron transfer involving $Ni^{2+}$/ $Ni^{3+}$ oxidation process.

Hence,

**The surface-active site of 2 that participated in OER = $2.96 \times 10^{16}$**

**For complex 3**

Calculated area associated with the oxidation peak = $0.01948 \times 10^{-3}$ V A

Hence the associated charge was = $0.01948 \times 10^{-3}$ V A / 0.005 V $s^{-1}$

$= 3.89 \times 10^{-3}$ As

$= 3.89 \times 10^{-3}$ C

Now, the number of electron transferred was = $3.89 \times 10^{-3}$ C / $1.602 \times 10^{-19}$ C

$= 2.43 \times 10^{16}$

The number of electron calculated above was same as the number of surface active site due to single electron transfer involving $Ni^{2+}$/ $Ni^{3+}$ oxidation process.

Hence,

**The surface-active site of 3 that participated in OER = $2.43 \times 10^{16}$**

**For complex 4**

Calculated area associated with the oxidation peak = $0.01043 \times 10^{-3}$ V A

Hence the associated charge was = $0.01043 \times 10^{-3}$ V A / 0.005 V $s^{-1}$

$= 2.08 \times 10^{-3}$ As

$= 2.08 \times 10^{-3}$ C

Now, the number of electron transferred was = $2.08 \times 10^{-3}$ C / $1.602 \times 10^{-19}$ C

$= 1.29 \times 10^{16}$

The number of electron calculated above was same as the number of surface active site due to single electron transfer involving $Ni^{2+}$/ $Ni^{3+}$ oxidation process.

Hence,

**The surface-active site of 4 that participated in OER = $1.29 \times 10^{16}$**

**Equation S2. Determination of Turn-Over Frequency (TOF)**

The TOF of the complexes can be determined using the equation:

$$TOF = (j \times N_A) / (4 \times F \times n)$$

Where, j = current density at 330 mV

$N_A$ = Avogadro number

F = Faraday constant

n = number of active Ni-sites

**For Complex 1:**

$TOF = [(2.12 \times 10^{-3}) (6.023 \times 10^{23})] / [(96485) (4) (0.88 \times 10^{16})]$

**$TOF = 3.7 \times 10^{-1}\ s^{-1}$**

**For Complex 2:**

$TOF = [(10.00 \times 10^{-3}) (6.023 \times 10^{23})] / [(96485) (4) (2.96 \times 10^{16})]$

**$TOF = 5.2 \times 10^{-1}\ s^{-1}$**

**For Complex 3:**

$TOF = [(4.78 \times 10^{-3}) (6.023 \times 10^{23})] / [(96485) (4) (2.43 \times 10^{16})]$

**$TOF = 3.0 \times 10^{-1}\ s^{-1}$**

**For Complex 4:**

$TOF = [(3.52 \times 10^{-3}) (6.023 \times 10^{23})] / [(96485) (4) (1.29 \times 10^{16})]$

**$TOF = 4.2 \times 10^{-1}\ s^{-1}$**

**Determination of faradaic efficiency**

The amount of oxygen generated during the oxygen evolution reaction was determined by the water displacement method. The amount of $O_2$ was detected during the chronoamperometric measurement for 1800 s at 20 mA $cm^{-2}$ current density.[1-3]

Firstly, the theoretical amount of $O_2$ was calculated using the following equation from Faraday's law.[1-3]

$$nO_2\,(\text{theoretical}) = \frac{Q}{n \times F} = \frac{I \times t}{n \times F} = \frac{0.02\ A \times 1800\ s}{4 \times 96485.3\ s\ A\ mol^{-1}} = 0.00093\ mmol$$

Where $nO_2$ denotes the theoretically calculated amount of $O_2$, Q is the amount of applied charge, *n* is the number of electrons participating in the OER reaction (4 electrons), *F* is the Faraday constant (96485.3 s A $mol^{-1}$), *I* is the applied current (0.02 A), and *t* is the reaction time (1800 s).

At the time of chronoamperometric measurements, the amount of $O_2$ produced during the experiment was measured and the theoretically calculated amount was compared with the actually generated amount of $O_2$. Further, the faradaic efficiency was calculated using the following equation:

$$\text{Faradaic efficiency}\,(\%) = \frac{nO_2\,(\text{experimental})}{nO_2\,(\text{Theoretical})} \times 100 = \frac{0.000915\ mmol}{0.00093\ mmol} \times 100 = 98.3\%$$

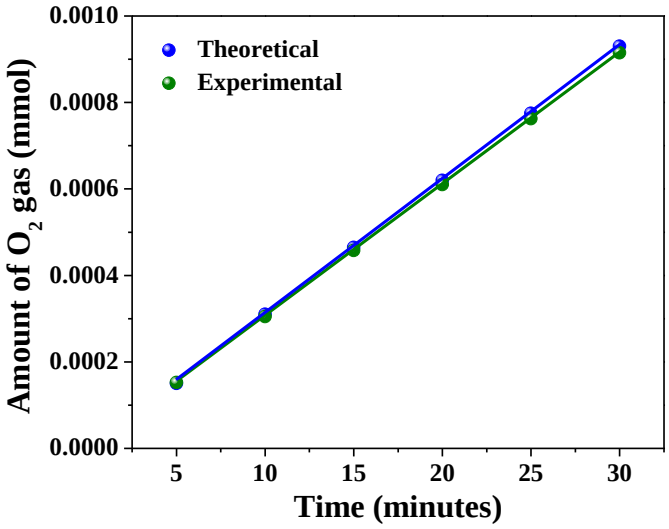


**Fig. S9.** Plot for the amount of theoretically calculated $O_2$ (blue line) and experimentally measured $O_2$ (green line) versus time for complex **2**.

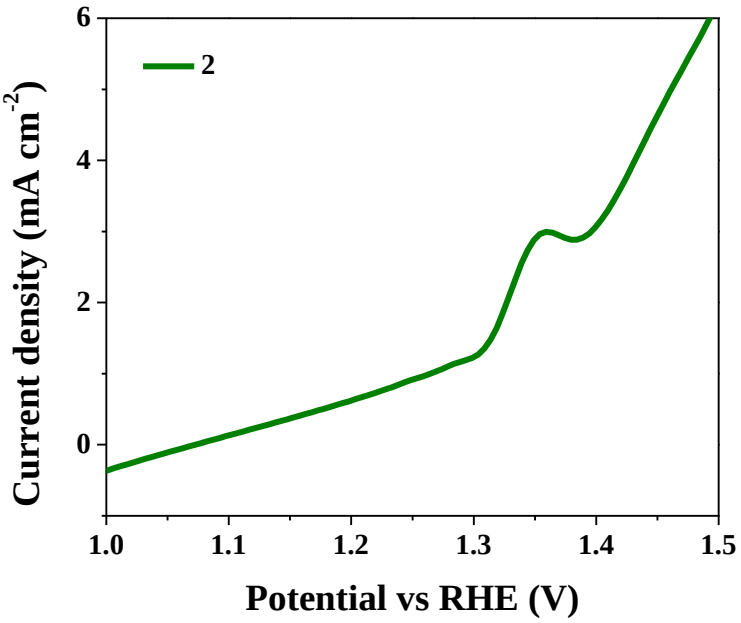


**Fig. S10:** Differential pulse voltammetric profile for the complex 2 utilized for the determination of number electron transferred for the redox peak.

The number of electrons could be calculated using DPV by the following equation at a constant pH.[4-5]

$$E_p - E_{p/2} = 2.218\ RT/nF = 57/n \quad \text{.....(1)}$$

Therefore, the equation (1) gives the number of electron transferred is

$$n = 57/\ E_p - E_{p/2}$$

where $E_p$ = peak potential of DPV

$E_{p/2}$ = potential at which half the peak current is observed

n = number of electron(s) transferred

From DPV, the Ep was calculated to be 1.357 V while $E_{p/2}$ was determined to be 1.313 V for complex **2**.

$$n = 57/\ 1.357\text{-}1.313$$

$$n = 57/\ 44$$

$$\mathbf{n = 1.29}$$

Therefore, the number of electron transferred for the redox peak is calculated to be one.

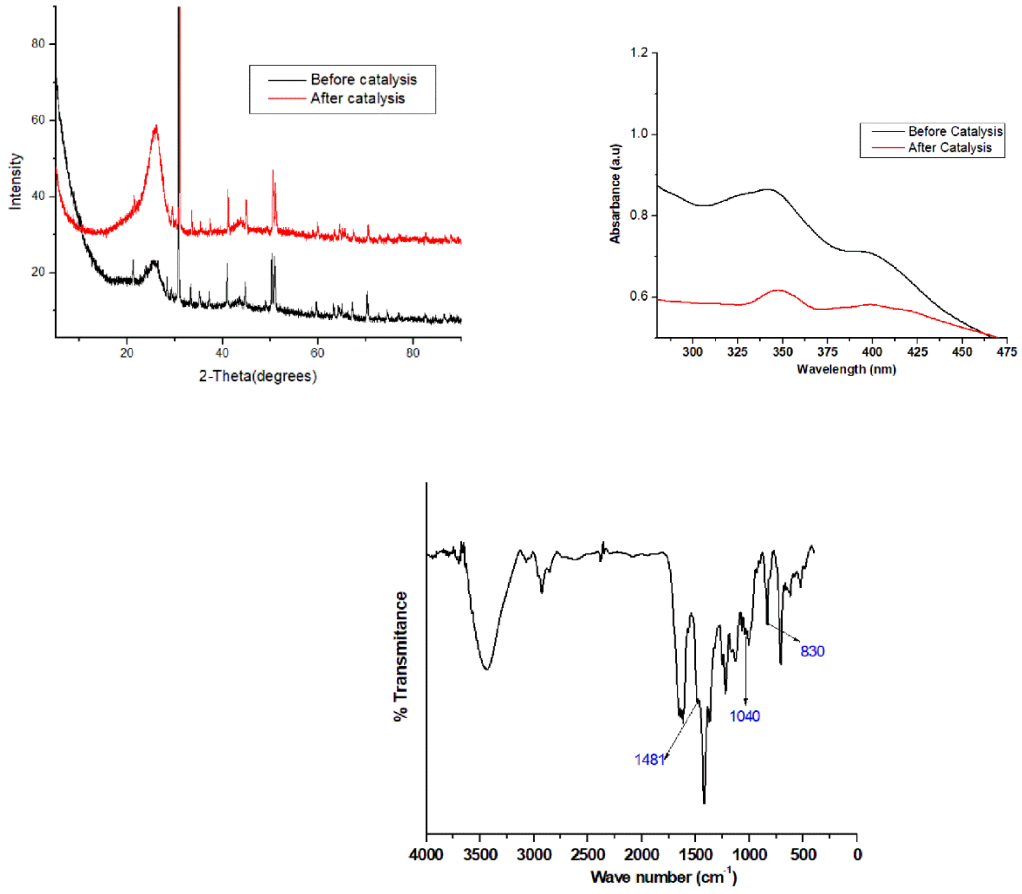


**Fig. S11:** (a) Powder XRD pattern of complex **2** and after 2 h OER catalysis indicating that the molecular structure was retained after 2 h OER catalysis (b) UV-vis. spectra of complex **2** before the OER and after the 2 h OER catalysis and (c) IR spectrum of complex **2** after 2 h OER catalysis indicating the new peak at 830 $cm^{-1}$ assigned for the Ni-O-Ni stretching in Ni(O)OH active catalyst.

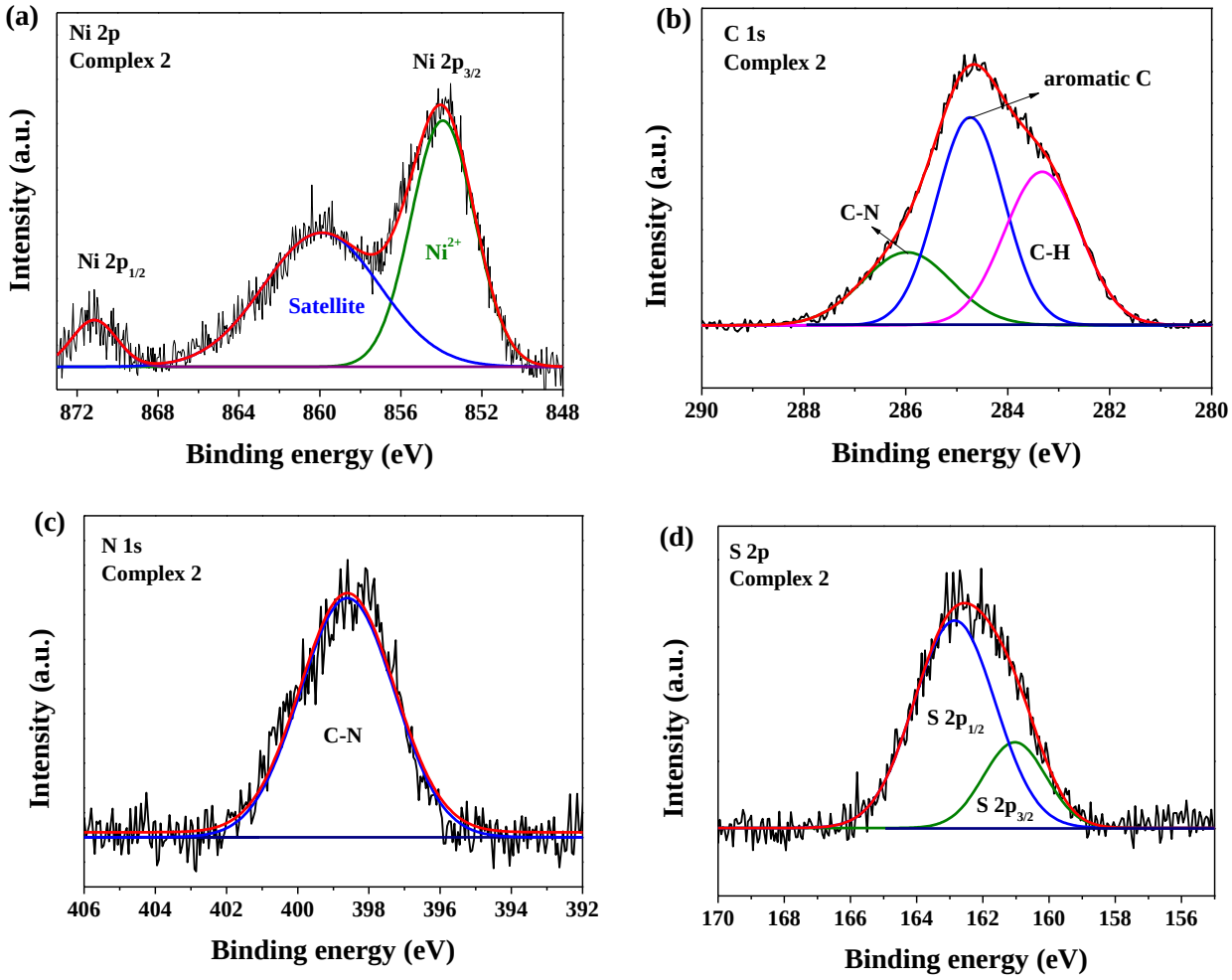


**Fig. S12:** (a) Ni 2p XPS of complex **2** showing the peaks at 853.8 eV and 871.1 eV assigned for the Ni2p$_{3/2}$ and Ni2p$_{1/2}$, respectively, the peak at 853.9 eV was attributed to the $Ni^{2+}$ species; (b) C 1s spectra of complex **2** showing three peaks at 285.9 eV, 284.5 eV, and 283.3 eV corresponded to the C-N bond, aromatic C and C-H bond, respectively; (c) C 1s spectra of complex **2** indicating the peak at 398.5 eV assigned for the N-C bond; and (d) S 2p XPS indicating two peaks at 161.0 eV and 162.9 eV attributed to the S 2p$_{3/2}$ and S 2p$_{1/2}$, respectively.

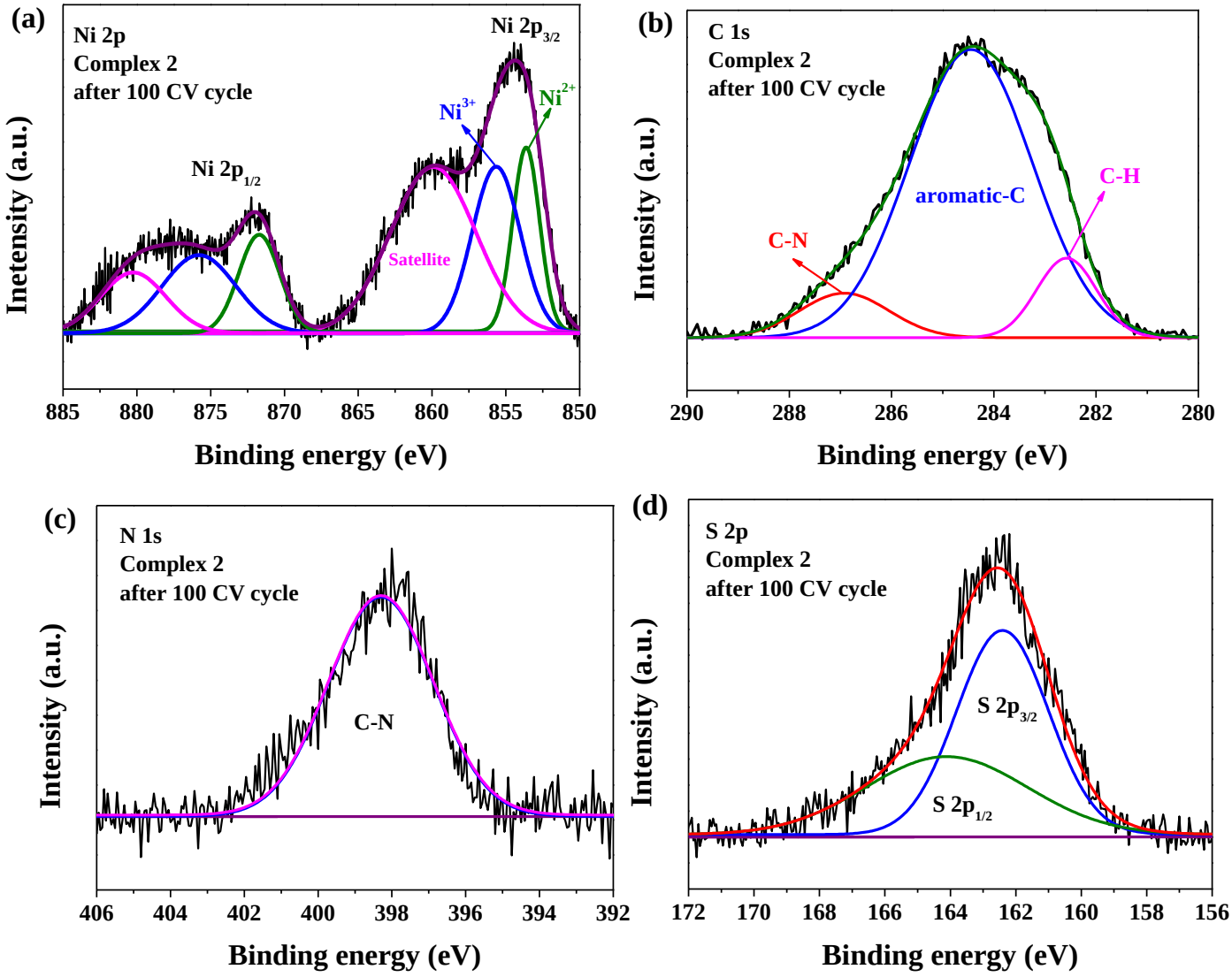


**Fig. S13:** (a) Ni 2p XPS of complex **2** showing the peaks at 854.4 eV and 871.8 eV assigned for the Ni2$p_{3/2}$ and Ni2$p_{1/2}$, respectively, the peak at 853.6 eV and 855.6 eV were attributed to the $Ni^{2+}$ and $Ni^{3+}$ species, respectively; (b) C 1s spectra of complex **2** showing three peaks at 286.9 eV, 285.0 eV and 283.6 eV corresponded to the C-N bond, aromatic C and C-H bond, respectively; (c) C 1s spectra of complex **2** indicating the peak at 398.3 eV assigned for the N-C bond; and (d) S 2p XPS indicating two peaks at 162.3 eV and 164.2 eV attributed to the S $2p_{3/2}$ and S $2p_{1/2}$, respectively.

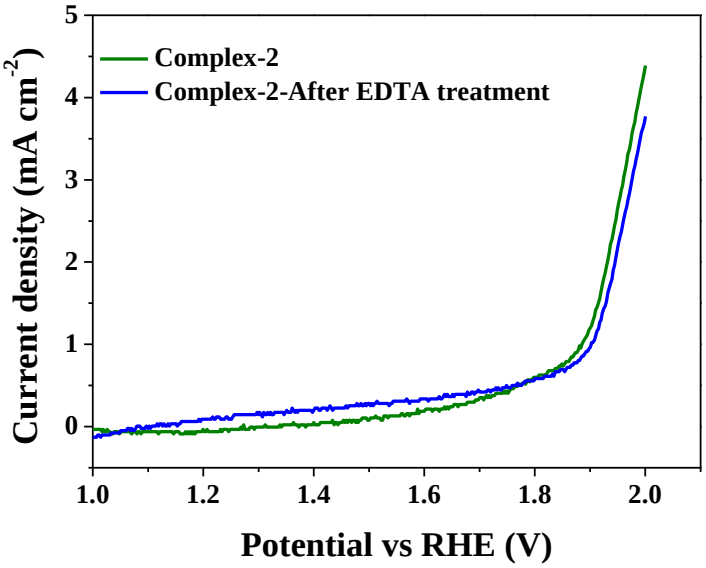


**Fig. S14:** LSV profiles for the oxygen evolution reaction of complex **2** before and after EDTA treatment. Complex **2** was activated first and treated with EDTA to remove the surface NiOOH. After the removal of surface NiOOH, LSV was recorded in phosphate buffer (pH 7).

**References**

1. J. Jia, L. C. Seitz, J. D. Benck, Y. Huo, Y. Chen, J. W. D. Ng, T. Bilir, J. S. Harris, T. F. Jaramillo, *Nat. Commun.* 2016, **7**, 13237.

2. A. Paracchino, V. Laporte, K. Sivula, M. Grätzel, E. Thimsen, *Nat. Mater*. 2011, **10**, 456-461.

3. I. M. Mosa, S. Biswas, A. M. El-Sawy, V. Botu, C. Guild, W. Song, R. Ramprasad, J. F. Ruslingace, S. L. Suib, *J. Mater. Chem. A* 2016, **4**, 620-631.

4. A.J. Bard, L.R. Faulkner, Electrochemical methods: fundamentals and applications, 2001, https://doi.org/10.1038/nprot.2009.120.Multi-stage.

5. D.A.C. Brownson, C.E. Banks, The handbook of graphene electrochemistry, 2014, https://doi.org/10.1007/978-1-4471-6428-9.